Preprints of the 19th World Congress
The International Federation of Automatic Control
Cape Town, South Africa. August 24-29, 2014

Energy Efficiency of Overhead Cranes

Zhou Wu, Xiaohua Xia

Department of Electrical Electronic Computer Engineering, University of Pretoria, Pretoria, SA (e-mail: wuzhsky@gmail.com, xxia@up.ac.za).

Abstract: Energy efficiency is firstly considered into the control of overhead cranes. Based on the model of crane system, energy consumption as well as operational safety is formulated in an optimal control problem. The optimal control is used to search optimal trajectories of velocity and acceleration for minimizing energy consumption. Existing related work mainly focused on reducing transportation time and swing, but trajectory in this paper focuses on increasing energy efficiency of transportation while satisfying practical and physical constraints. Model predictive control (MPC) is then proposed to track optimal trajectories in real-time. As a result, the actual trajectories can match the reference trajectories with small errors when external disturbances exist. In the simulation, it can be shown that the proposed control approach can improve energy efficiency of overhead cranes robustly.

Keywords: crane control, motion planning, model predictive control, tracking, energy efficiency.

1. INTRODUCTION

Due to high payload capacity, good operational flexibility and transportation efficiency, overhead cranes have been widely used in many industrial fields, such as sea ports, construction sites, manufacturing plants and factories (Peng et al., 2012; Ngo and Hong, 2012). Regardless of the type of overhead crane, each crane always has a similar fundamental structure that can be described as a trolley-pendulum system, that consists of a trolley, a supporting frame and a rope connecting the trolley with the payload. The crane system has one control input (trolley's actuating force) and two system variables to be controlled (trolley's position and payload's swing angle). It is difficult to control this so-called underactuated mechanical system that has fewer independent control inputs than degrees of freedom. Therefore, the automatic control of crane has attracted much interest from researchers in areas of mechanics and control.

Under the assumption of small payload swing, the nonlinear model of crane can be linearized around its equilibrium points, and then linear control approaches can be used on the simplified linear system. Many linear control methods have been applied to overhead cranes, including feedback control (Hekman and Singhose, 2006), input shaping (feedforward control) (Singhose et al., 2000; Garrido et al., 2008), optimal control (Moon et al., 1996; Piazzi and Visioli, 2002; Terashima et al., 2007). Time efficiency is the main objective of crane control that is usually considered in previous work (Chang and Wijaya Lie, 2012; Sun et al., 2012a). In Moon et al. (1996), time optimal control theory has been evaluated on the bang-bang control system of cranes. In Piazzi and Visioli (2002); Terashima et al. (2007), time optimal trajectories have been designed for continuous system of cranes subject to the swing constraint.

Two important issues have been neglected, i.e., energy efficiency and safety, which turn out to be significantly urgent when a large number of cranes have been equipped in some international industrial fields. To the best of our knowledge, little work has been done to minimize the swing risk while most work only considered the swing as a constraint of the control problem. The total energy consumption, has seldom been optimized in crane control, because the relation between energy consumption and control sequence is still vague. In this paper, energy efficiency as well as safety will be considered in the proposed control approach, that includes trajectory planning and tracking. Optimal trajectories in terms of energy efficiency and safety are planned by the optimal control method. As references, these optimal trajectories will be tracked in real time by model predictive control (MPC).

The reminder of this paper is organized as follows. Section 2 presents the dynamic model of overhead cranes. The discrete-time model is deduced in Section 3. Section 4 illustrates our control approach. Section 5 shows results of numerical simulation. Conclusion is given at last.

2. DYNAMIC MODEL OF OVERHEAD CRANES

The structure of an overhead crane can be illustrated as shown in Figure 1, where the trolley moves on the horizontal bridge and the payload is connected with a constant-length rope. $x(t)$, $\theta(t)$ and $F(t)$ denote the trolley's position, the payload's swing angle and overall force on the trolley respectively. In this paper, air resistance as well as stiffness and mass of the rope is neglected and the load is considered as a point mass. Moreover, as this study only focuses on the control of horizontal transportation, hoisting and lowering of payload are not considered. Then the overhead crane system with constant rope length can be described as follows:

$$(M+m)\,\ddot{x} + ml\cos\theta\ddot{\theta} - ml\sin\theta\dot{\theta}^2 = F, \qquad (1)$$

$$ml^2\ddot{\theta} + ml\cos\theta\ddot{x} + mgl\sin\theta = 0, \quad (2)$$

where M and m denote masses of the trolley and the payload, respectively. l is the length of the rope; g is the gravitational acceleration. The overall force F is composed of the actuating force F_a and the friction F_r as

$$F = F_a - F_r, \quad (3)$$

$$F_r \propto (M+m)g, \quad (4)$$

Motivated by the friction models in Makkar et al. (2007); Sun et al. (2012b), this paper employs the friction model as

$$F_r = (k_{r1}\tanh\dot{x}/\xi + k_{r2}|\dot{x}|\dot{x})(M+m)g, \quad (5)$$

where k_{r1}, k_{r2} and ξ are friction-related coefficients that can be determined by offline regression of historical data.

The crane dynamics consist of the actuated part (Eq. (1)) and the underactuated part (Eq. (2)). The latter part is the system kinematics that defines the coupling behavior between the trolley's acceleration $\ddot{x}(t)$ and the payload's swing angle $\theta(t)$. The main difficulty in controlling the overhead crane lies in handling of the coupling behavior between the swing and horizontal motion. When the swing angle is small enough ($\theta(t) < 5°$), the kinematic equation (2) can be linearized with the approximations of $\cos\theta \simeq 1$ and $sin\theta \simeq \theta$. The approximated linear kinematics can be obtained as

$$l\ddot{\theta} + \ddot{x} + g\theta = 0. \quad (6)$$

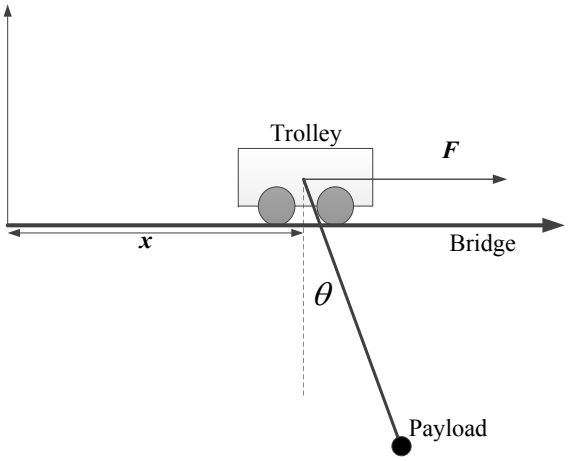

Fig. 1. Two-dimensional overhead crane system

In the evaluated time interval $[0, T]$, the crane is required to arrive at the destination without residual swing. Therefore, several principles must be satisfied according to the physical and practical situations in crane control.

Principle 1: The trolley reaches the desired location p_d at the end of the period. The final states must ensure that the trolley is static with no swing and that it can be lowered immediately as

$$x(T) = p_d, \dot{x}(t) = 0, \theta(T) = 0, \dot{\theta}(T) = 0. \quad (7)$$

Principle 2: During the horizontal transportation, the velocity and acceleration of the trolley must be limited in certain ranges as

$$\begin{cases} 0 \le \dot{x}(t) \le v_m, & t \le T \\ |\ddot{x}(t)| \le a_m, & t \le T \end{cases}, \quad (8)$$

where v_m and a_m are the permitted limits of velocity and acceleration, respectively.

Principle 3: The payload swing during the transportation must be limited within a safe range as

$$|\theta(t)| \le \theta_m, t \le T, \quad (9)$$

where θ_m is the permitted maximum of swing amplitude.

Principle 4: The jerk (defined as the time derivative of acceleration $j(t) = \dddot{x}(t)$) must be limited to a reasonable range to satisfy the mechanical constraint and to prolong the motor's lifetime.

$$|j(t)| \le j_m, t \le T \quad (10)$$

where j_m is the permitted maximal jerk in the horizontal transportation.

3. DISCRETE MODEL OF OVERHEAD CRANES

In our proposed approach, the sequence of control input is $[F_a(1), F_a(2), \ldots, F_a(N)]^T$, where $F_a(n)$ is the actuating force at the nth sampling period and N is the total number of samples in the planning period T. Therefore, the continuous system need be discretized by a sampling period t_0. The discrete model of overhead cranes can be formulated as Eq. (11) and (12).

$$(M+m)\,a(n) + ml\cos\theta(n)\ddot{\theta}(n) - ml\sin\theta(n)\dot{\theta}(n)^2 = F(n), \quad (11)$$

$$l\ddot{\theta}(n) + a(n) + g\theta(n) = 0, \quad (12)$$

where $N = T/t_0$ and $n = 1, \ldots, N$; $a(n)$ and $F(n)$ represent acceleration and overall force at the nth sample respectively. $\theta(n)$, $\dot{\theta}(n)$ and $\ddot{\theta}(n)$ are measured swing angle, swing velocity and swing acceleration at the nth sample. At the period $[n-1, n)$, the overall force $F(n)$ is composed of the actuating force $F_a(n)$ and the friction $F_r(n)$ as

$$F(n) = F_a(n) - F_r(n), \quad (13)$$

where the friction $F_r(n)$ can be formulated similarly with Eq. (5) as

$$F_r = [k_{r1}\tanh\dot{x}(n)/\xi + k_{r2}|\dot{x}(n)|\dot{x}(n)](M+m)g. \quad (14)$$

In this discrete model, we denote the vector of acceleration as $\boldsymbol{a}$ ($a(n) = \Delta^2 x(n)$), and denote the vector of velocity as $\boldsymbol{v}$ ($v(n) = \Delta x(n)$). Suppose that the initial position is $x(0)$, the initial velocity is $v(0)$, the initial acceleration is $a(0)$, the initial swing angle is $\theta(0)$, and the initial swing velocity is $\dot{\theta}(0)$. Given an vector of acceleration $\boldsymbol{a}$, the velocity $\boldsymbol{v}$ and the displacement $\boldsymbol{x}$ can be expressed as

$$\begin{cases} \boldsymbol{v} = \boldsymbol{v}_0 + \boldsymbol{A}\boldsymbol{a}t_0^2 \\ \boldsymbol{x} = \boldsymbol{x}_0 + \boldsymbol{b}v(0)t_0 + \boldsymbol{A}_x\boldsymbol{a}t_0^2 \end{cases}, \quad (15)$$

where

$$\boldsymbol{v}_0 = [\overbrace{v(0), ..., v(0)}^{N}]^T, \quad (16)$$

$$\boldsymbol{x}_0 = [x(0), ..., x(0)]^T, \quad (17)$$

$$\boldsymbol{b} = [1, 2, \ldots, N]^T, \quad (18)$$

$$\boldsymbol{A} = \begin{bmatrix} 1 & 0 & 0 & \dots & 0 \\ 1 & 1 & 0 & \dots & 0 \\ 1 & 1 & 1 & \ddots & 0 \\ \vdots & \vdots & \vdots & \ddots & \vdots \\ 1 & 1 & 1 & \dots & 1 \end{bmatrix}, \tag{19}$$

$$\boldsymbol{A}_x = \begin{bmatrix} 0.5 & 0 & 0 & \dots & 0 \\ 1.5 & 0.5 & 0 & \dots & 0 \\ 2.5 & 1.5 & 0.5 & \ddots & 0 \\ \vdots & \vdots & \vdots & \ddots & \vdots \\ N-0.5 & N-1.5 & N-2.5 & \dots & 0.5 \end{bmatrix}. \tag{20}$$

According to initial states, the swing angle $\boldsymbol{\theta}$ can be formulated as

$$\boldsymbol{\theta} = \theta(0)\cos(\boldsymbol{b}w_n t_0) + \frac{\dot{\theta}(0)}{w_n}\sin(\boldsymbol{b}w_n t_0) + A_\theta \boldsymbol{a}t_0^2, \tag{21}$$

where $w_n = \sqrt{g/l}$ is the natural frequency of system. Note that sine and cosine functions are calculated on each component of $\boldsymbol{b}w_n t_0$. In Eq. (21) the first two components at the right hand side is the initial-conditions response and the third component is the forced response. Based on the kinematic Eq. (12), the matrix $\boldsymbol{A}_\theta$ can be formulated as

$$\begin{aligned} \boldsymbol{A}_\theta &= -\frac{1}{l}\boldsymbol{C}^{-1} \\ &= -\frac{1}{l}\begin{bmatrix} 1+gt_0/l & 0 & 0 & \dots & 0 & 0 & 0 \\ -2 & 1+gt_0/l & 0 & \dots & 0 & 0 & 0 \\ 1 & -2 & 1+gt_0/l & \ddots & 0 & 0 & 0 \\ 0 & \dots & \ddots & \ddots & \ddots & \ddots & \vdots \\ 0 & \dots & \ddots & \ddots & 1 & -2 & 1+gt_0/l \end{bmatrix}^{-1} \end{aligned} \tag{22}$$

Note that the matrix $\boldsymbol{C}$ is non-singular. It can be noticed in Eq. (15) and Eq. (21) that state variables are calculated at the initial time. At the kth sample, calculations of future states have similar expressions with Eq. (15) and Eq. (21), which can be generalized as

$$[x(i), v(i), \theta(i), \dot{\theta}(i)]^T = \mathrm{g}(i, [x(k), v(k), \theta(k), \dot{\theta}(k)]^T) \tag{23}$$

where $k+1 \le i \le N$, $x(k)$, $v(k)$, $\theta(k)$ and $\dot{\theta}(k)$ represent current state variables.

Based on this discrete model, our control approach, including trajectory planing and tracking, is proposed to optimize energy efficiency of transportation. When the profile of acceleration is planned, the profiles of velocity and swing are determined. As a result, the actuating force is determined according to Eq. (11),(13), and (14). In other words, the profile of force can be represented with the profile of acceleration using some simple transformations.

4. THE PROPOSED CONTROL APPROACH

Energy efficiency and safety have been considered in our approach. This approach can be divided into two steps, i.e. trajectory planning and tracking as shown in Fig. 2. For trajectory planning, an objective function is made to quantify energy efficiency and safety. The optimal control theory is then employed to search an optimal trajectory for minimizing the objective function. For trajectory tracking, MPC is employed to control the crane following the planned trajectory while satisfying all practical constraints. Note that the horizon of MPC is receded at each control period. The aim of tracking is to minimize difference between the reference and predicted trajectories over the future horizon.

4.1 Trajectory planning

Operational safety can be reflected by two metrics, i.e. the maximal swing angle and the residual swing. After integrating these two metrics, safety can be formulated as

$$J_{11}(\boldsymbol{a}) = \alpha \max_{n\in\{1,\dots,N\}} \theta(n) + (1-\alpha)\sum_{n=N-N_r+1}^{N} \frac{\theta(n)}{N_r} \tag{24}$$

where N_r is the number of samples considered in the residual swing. The first component of the right-hand side is the maximal swing angle, and the second component of the right-hand side is the residual swing. The coefficient α is used to integrate these two metrics. α is set to 0.5 in this paper. Note that residual swing is defined as the average swing angle during the final $N_r \cdot t_0$ period.

Within the planning period T, energy consumption for the horizontal transportation can be calculated as

$$E = \int_0^T P dt = \int_0^T F_a \dot{x} dt \tag{25}$$

where F_a is output force of the actuating motor, P is power of the actuating motor, and E is energy consumption of the motor. For the discrete system, energy consumption is similarly formulated as

$$J_{12}(\boldsymbol{a}) = \sum_{n=1}^{N} F_a(n)v(n) = \sum_{n=1}^{N} [F(n) + F_r(n)]v(n) \tag{26}$$

where the overall force $F(n)$ is computed as Eq. (11), and the friction $F_r(n)$ can be computed as Eq. (14).

Therefore, the objective function for trajectory planning will integrate safety and energy consumption as

$$J_1(\boldsymbol{a}) = \beta J_{11} + (1-\beta)J_{12} \tag{27}$$

where the integrating parameter β is set as 0.99 in this paper.

By substituting $v(n)$ and $\theta(n)$ with $a(n)$ using Eq. (15) and Eq. (21), the objective function can be expressed by the acceleration $\boldsymbol{a}$. Note that the profile of actuating force is indirectly computed by the planned profile of acceleration in this paper. The planned acceleration $\boldsymbol{a}$ is bounded in the range $[-a_m, a_m]$ as

$$a(n) \in [-a_m, a_m], n = 1, \dots, N. \tag{28}$$

The constraints include the equality constraints, such as terminate states of displacement, velocity and swing angle; and also include the inequality constraints, such as limits of velocity, swing angle and jerk. The set of constraints is formulated as

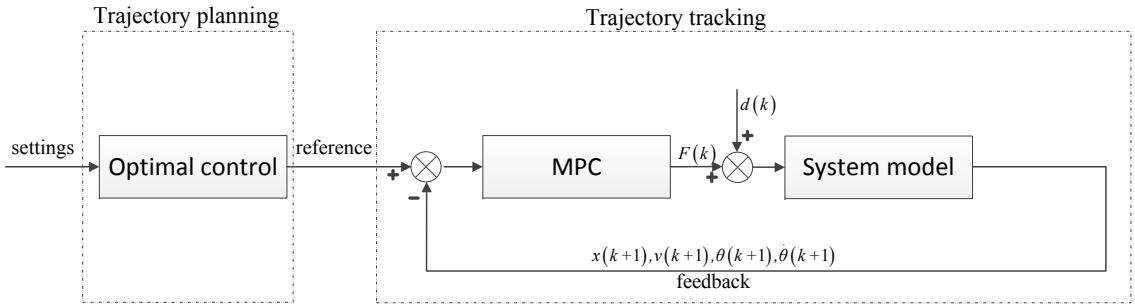

Fig. 2. Structure of the proposed control approach

$$\mathcal{C}(k): \begin{cases} -a_m \le a(n) \le a_m, & n = k+1, \dots, N \\ x(N) = x_p \\ v(N) = 0 \\ \theta(N) = 0 \\ \theta(N-1) = 0 \\ 0 \le v(n) \le v_m, & n = k+1, \dots, N \\ |\theta(n)| \le \theta_m, & n = k+1, \dots, N \\ |a(n+1) - a(n)| \le j_m, & n = k+1, \dots, N-1 \\ |a(1)| \le j_m \\ |a(N)| \le j_m \end{cases} . \tag{29}$$

where $\mathcal{C}(k)$ represents the set of constraints over the interval $[k, N), k = 0, \dots, N-1$. Note that for trajectory planning $k = 0$ and the required constraints are $\mathcal{C}(0)$.

When minimizing the objective function Eq. (27) under the constraints $\mathcal{C}(0)$, the optimal profiles of acceleration, velocity and force will be found. The trajectory obtained is expected to have high degree of safety and low energy consumption.

4.2 Trajectory tracking

In MPC, another objective function is required to evaluate the error of tracking at each sampling instant. At the kth sampling instant, the tracking error over the interval $[k, N)$ can be expressed as

$$J_2 = \sum_{n=k+1}^{N} [v(n) - v_r(n)]^2 + \gamma \sum_{n=k+1}^{N} [\frac{\theta(n) - \theta_r(n)}{\cos\theta_r(n)}]^2, \tag{30}$$

where $k = 1, \dots, N-1$ is the current instant; $v_r(n)$ and $\theta_r(n)$ are the references of velocity and swing angle; $v(n)$ and $\theta(n)$ are the predicted state variables of velocity and swing angle. γ is the weighting parameter for integration. The first component at the right hand side is the tracking error of velocity, and the second component is the tracking error of swing. The weight γ is set to 10 in this paper.

By substituting $v(n)$ and $\theta(n)$ with $a(n)$ using Eq. (23), the objective function can be expressed by acceleration. The acceleration $a(n)$ must be bounded in $[-a_m, a_m]$, and the constraints in MPC are $\mathcal{C}(k)$.

In MPC, the optimal control problem in the horizon $[k, N)$ is repeatedly solved ($k = 1, \dots, N-1$). Using the optimal solution obtained, the input force is calculated and applied to the system. The optimal control problem, say the objective function and the set of constraints, has been defined in Eq. (30) and (29). At the kth sample, an optimal solution $[a(k+1), a(k+2), \dots, a(N)]^T$ can be obtained after solving the optimal problem. Then the control input $[F_a(k+1), F_a(k+2), \dots, F_a(N)]^T$ will be computed based on the system model. $F_a(k+1)$ is applied to the system in the period $[k, k+1)$. The procedure of MPC approach can be illustrated as follows.

Set $k = 0$;
while $k < N$ **do**
  Measure current state variables $x(k), v(k), \theta(k), \dot{\theta}(k)$;
  Solve the optimal control problem Eq. (30) subject to Eq. (29);
  For the optimal solution $[a(k+1), a(k+2), \dots, a(N)]^T$, calculate the control input $[F_a(k+1), F_a(k+2), \dots, F_a(N)]^T$;
  Apply $F_a(k+1)$ to the system at the period $[k, k+1)$;
  $k = k + 1$;
end

Algorithm 1. MPC for trajectory tracking

It can be noticed that the reference trajectory designed in the first step of planning is required in MPC. At each sampling instant, the horizon of the optimal control problem will be decreased by one. In each interval $[k, k+1)$, displacement, velocity, swing angle and swing velocity are measured. If there is any disturbance in the previous period $[k-1, k)$, the optimal MPC controller will make the compensation and correction automatically. For this reason, the closed-loop nature of MPC comes with an inherent property of robustness.

5. NUMERICAL SIMULATION

The overhead crane system described in Sun et al. (2012a) is used to test our proposed approach. The physical parameters of the system are listed as follows

$$m = 1.025\text{kg}, M = 7\text{kg}, l = 0.75\text{m}, g = 9.8\text{m/s}^2. \tag{31}$$

The desired trolley location in simulation is set as $p_d = 1.5$m, and the practical constraints are given as

$$v_m = 0.4\text{m/s}, a_m = 0.2\text{m/s}^2, \theta_m = 5^\circ, j_m = 2\text{m/s}^3. \tag{32}$$

The parameters for the friction model Eq. 5 are referred from the results of offline regression in Sun et al. (2012b) as

$$k_{r1} = 0.5483, \xi = 0.01, k_{r2} = 0.0623. \tag{33}$$

Test 1: trajectory planning

The evaluated planning period T is 7s, and the sampling period t_0 is 0.1s. The duration of residual swing is defined

Table 1. Comparisons of swing

Swing metrics	Optimal trajectory	Trajectory 1	Trajectory 2	Trajectory 3	Trajectory 4
Maximal swing (°)	1.126	1.936	2.004	2.002	2.002
Residual swing (°)	0.721	0.893	0.869	0.88	0.876
Average (°)	**0.923**	1.414	1.436	1.440	1.439

Table 2. Comparisons of energy efficiency

Energy metrics	Optimal trajectory	Trajectory 1	Trajectory 2	Trajectory 3	Trajectory 4
Energy usage (J)	6.695	6.676	6.651	6.653	6.653
Peak power (W)	1.698	1.975	1.678	1.602	1.589

as the last 2s, i.e., $N_r = 20$. The optimization algorithm for solving the planning problem is chosen as the *fmincon* function in Matlab toolbox. Note that *fmincon* is a simple example of solver in our simulation, other more complicated solvers may also be employed instead of it here. In the *fmincon* function, the algorithm type is set as "interior-point"and the maximum function evaluation times are $50 \cdot N$.

As the scope is limited in the motion planning methods, four trajectory references mentioned in Lee (2005) (trajectory 1),Sun et al. (2012a) (trajectory 2, 3 and 4) are chosen in comparison in this section. For the same specific overhead system, we have plotted these four trajectories and our planned optimal trajectory in Fig. 3. For each trajectory, the profiles of velocity, acceleration and swing angle are shown in the figure.

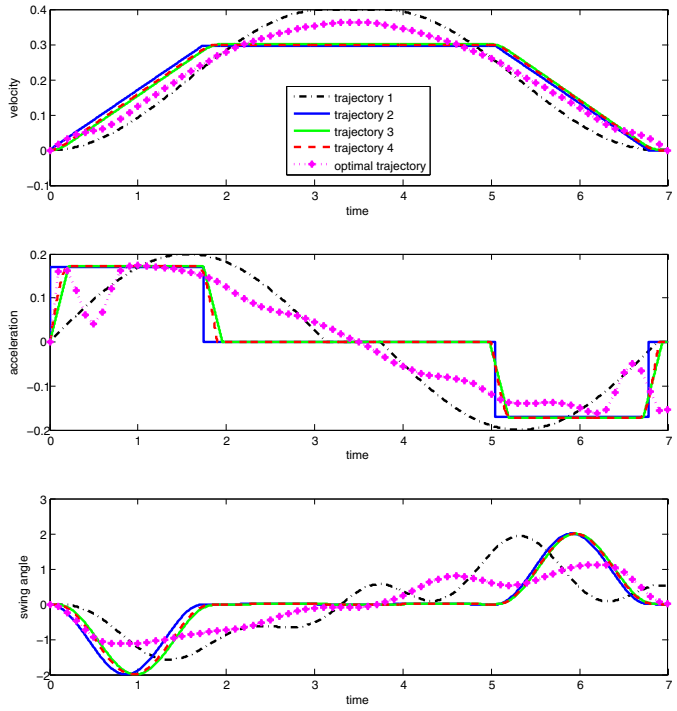

Fig. 3. Profiles of velocity, acceleration and swing angle

For each trajectory, the results of maximum swing angle, residual swing and their average are listed in Table 1. For the optimal trajectory, the maximal swing angle is the smallest as 1.126°, and the residual swing and the average swing are also smallest among the compared trajectories. In Fig. 3, the profiles of velocity, acceleration and swing angle are given. Due to the constraint of jerk, acceleration and deceleration are smooth in the optimal trajectory. In Fig. 3, it can be noticed that the maximum swing angles are smallest and the residual swing is close to zero.

In Table 2, energy consumption and peak power over the planning period are listed for each trajectory. For the optimal trajectory, energy consumption and peak load are not the smallest. One possible reason is that other trajectories have less constraints than the optimal trajectory. For example, the constraint of jerk is only considered in our planning method. Another reason is that the weight $\beta = 0.99$ is chosen in the objective function, which is set as a trade-off between energy efficiency and safety. When $\beta = 0$ is used, our method can obtain an ideal trajectory with the smallest energy consumption 6.649 J and the smallest peak power 1.36 W.

Test 2: trajectory tracking

In this part, MPC is used to track the reference trajectory obtained from Test 1 as shown in Fig. 3. To validate stability and robustness of the tracking method, random disturbances are added to the actuating force between 1s and 3s as

$$\begin{cases} F_a(n) = F(n) + F_r(n) + d(n) \\ d(n) = rand - 0.5 \end{cases}, 10 \le n \le 30, \qquad (34)$$

where *rand* is a random number uniformly distributed in $[0, 1]$. The referenced and disturbed profiles of force have been shown in Fig. 4. The open-loop control method using the referenced profile of force is included in the following comparison. For the open-loop control and MPC, the performance in terms of tracking error of velocity and swing angle is given in Table 3.

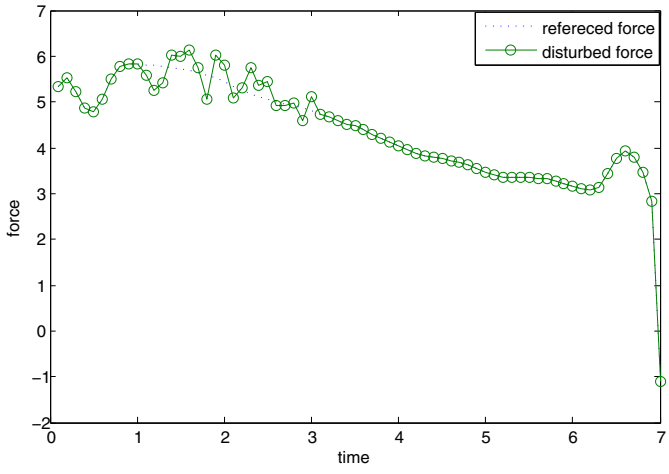

Fig. 4. Profiles of referenced and disturbed control inputs

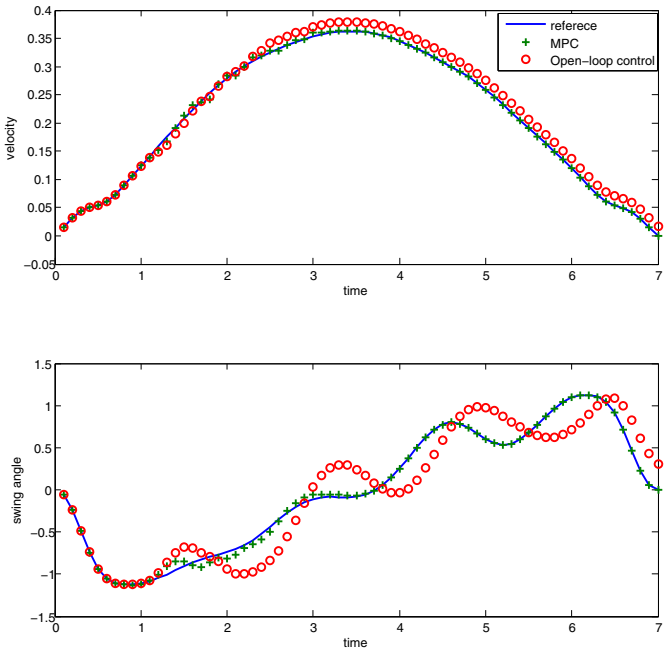

Fig. 5. Comparison between MPC and the open-loop control

Table 3. Comparisons of tracking error

Tracking error	Open-loop control	MPC
Velocity (m/s)	0.0136	0.0028
Swing angle (°)	0.249	0.032

At the presence of disturbances, it can be noticed that tracking errors of MPC are much smaller than errors of open-loop control. For MPC, the tracking error of velocity is 0.0136m/s, and the tracking error of swing is 0.032°. The profiles of velocity and swing angle have been shown in Fig. 5. For MPC, velocity and swing angle have been tracked with small errors over the transportation period. Meanwhile, it is worth noting that the results of MPC can satisfy the constraints, such as zero final velocity and zero final swing, which cannot be achieved by the open-loop control.

6. CONCLUSION

In this paper, energy efficiency is firstly modeled in crane control while considering many practical and physical constraints, including maximal swing and jerk. Two steps of control, i.e. trajectory planning and tracking, are proposed to minimize energy consumption of transportation. Using the proposed trajectory planning method, an optimal trajectory with small swing and low energy consumption can be obtained. The optimal trajectory obtained by off-line computation can be utilized as inputs of open-loop control schemes or references of closed-loop control schemes.

In practise, cranes are usually operated in the environment with disturbances. MPC is used to track the planned trajectory as the second step of our approach. The experimental results have been shown that MPC has smaller tracking errors than open-loop control. MPC has achieved great performance of stability and robustness when external disturbances exist. In future work, mechanism of online update may be considered in the optimal trajectory, and other closed-loop methods may be considered for tracking the planned trajectory.

REFERENCES

Chang, C.Y. and Wijaya Lie, H. (2012). Real-time visual tracking and measurement to control fast dynamics of overhead cranes. *IEEE Transactions on Industrial Electronics*, 59(3), 1640–1649.

Garrido, S., Abderrahim, M., Gimenez, A., Diez, R., and Balaguer, C. (2008). Anti-swinging input shaping control of an automatic construction crane. *IEEE Transactions on Automation Science and Engineering*, 5(3), 549–557.

Hekman, K. and Singhose, W. (2006). Feedback control for suppression of crane payload oscillation using on-off commands. In *Proceedings of the 2006 American Control Conference, 2006*, 1784–1789.

Lee, H.H. (2005). Motion planning for three-dimensional overhead cranes with high-speed load hoisting. *International Journal of Control*, 78(15), 875–886.

Makkar, C., Hu, G., Sawyer, W.G., and Dixon, W. (2007). Lyapunov-based tracking control in the presence of uncertain nonlinear parameterizable friction. *IEEE Transactions on Automatic Control*, 52(10), 1988–1994.

Moon, M., Vanlandingham, H., and Beliveau, Y. (1996). Fuzzy time optimal control of crane load. In *Proceedings of the 35th IEEE Conference on Decision and Control, 1996*, volume 2, 1127–1132 vol.2.

Ngo, Q.H. and Hong, K.S. (2012). Sliding-mode antisway control of an offshore container crane. *IEEE/ASME Transactions on Mechatronics*, 17(2), 201–209.

Peng, K., Singhose, W., and Gurleyuk, S. (2012). Initial investigations of hand-motion crane control with double-pendulum payloads. In *Proceedings of the 2012 American Control Conference, 2012*, 6270–6275.

Piazzi, A. and Visioli, A. (2002). Optimal dynamic-inversion-based control of an overhead crane. *IEE Proceedings of Control Theory and Applications*, 149(5), 405–411.

Singhose, W., Porter, L., Kenison, M., and Kriikku, E. (2000). Effects of hoisting on the input shaping control of gantry cranes. *Control Engineering Practice*, 8(10), 1159 – 1165.

Sun, N., Fang, Y., Zhang, X., and Yuan, Y. (2012a). Transportation task-oriented trajectory planning for underactuated overhead cranes using geometric analysis. *IET Control Theory Applications*, 6(10), 1410–1423.

Sun, N., Fang, Y., Zhang, Y., and Ma, B. (2012b). A novel kinematic coupling-based trajectory planning method for overhead cranes. *IEEE/ASME Transactions on Mechatronics*, 17(1), 166–173.

Terashima, K., Shen, Y., and Yano, K. (2007). Modeling and optimal control of a rotary crane using the straight transfer transformation method. *Control Engineering Practice*, 15(9), 1179 – 1192.